Competition between the Effects of Asymmetries in Ion Diameters and Charges in an Electrical Double Layer Studied by Monte Carlo Simulations and Theories

ARTICLE *in* THE JOURNAL OF PHYSICAL CHEMISTRY B · OCTOBER 2004

Impact Factor: 3.3 · DOI: 10.1021/jp0473873

3 AUTHORS, INCLUDING:

Mónika Valiskó
University of Pannonia, Veszprém
37 PUBLICATIONS **692** CITATIONS
SEE PROFILE

Dezso Boda
University of Pannonia, Veszprém
125 PUBLICATIONS **2,838** CITATIONS
SEE PROFILE

Competition between the Effects of Asymmetries in Ion Diameters and Charges in an Electrical Double Layer Studied by Monte Carlo Simulations and Theories

Mónika Valiskó

Department of Physical Chemistry, University of Veszprém, PO Box 158, H-8201 Veszprém, Hungary

Douglas Henderson*

Department of Chemistry and Biochemistry, Brigham Young University, Provo, Utah 84602

Dezső Boda

Department of Physical Chemistry, University of Veszprém, PO Box 158, H-8201 Veszprém, Hungary

Received: June 16, 2004; In Final Form: August 16, 2004

The electrical double layer near a charged electrode formed by a binary electrolyte in which the cations and anions have different diameters varying between 1.5 and 4.25 Å is studied by Monte Carlo (MC) simulation. Our emphasis is on small electrode charge, where new phenomena may be expected. As one would expect, there is a nonzero potential at the point of zero charge (PZC). Such an effect is outside the popular Gouy−Chapman theory, although it can be introduced. It arises naturally in the mean spherical approximation (MSA). A comparison of the simulation results is made with the linearized modified Gouy−Chapman (LMGC) and MSA. Surprisingly, for monovalent ions, the LMGC theory yields more reliable electrode potentials than does the MSA. In the case when the cations and anions have different charge, a nonzero PZC potential results, even if the diameters of the ions are equal. This phenomenon is not reproduced by either of the theories but is predicted by the modified Poisson−Boltzmann (MPB5) theory. Results are presented for the competition of the effects resulting from the size and charge asymmetries of the ions. A comparison of the density and potential profiles, as obtained from MC and LMGC calculations, is reported.

1. Introduction

The electrical double layer (DL) is formed by charged particles near a charged electrode. The conventional theory of the DL is that of Gouy[1] and Chapman (GC),[2] despite the fact that it is based on the questionable assumption that the diameters of the ions may be ignored.

The modern theory of the DL began with the use of the mean spherical approximation (MSA) by Blum[3] and the Monte Carlo (MC) simulations of Torrie and Valleau in a series of important papers.[4−9] They have taken into account several aspects, such as image effects,[5,8,9] ions with higher valence,[7,9] and ions with different diameters and/or a different distance of closest approach (DCA) to the electrode.[6,8] They considered ions at room temperature, whose diameter usually was 4.25 Å. They found that the GC theory was better for monovalent ions[4] than for divalent ions.[7]

Moreover, their simulations have served as a gold standard for subsequent theoretical work, such as the modified Poisson−Boltzmann theory (MPB),[10] the hypernetted chain (HNC) approximation,[11,12] integral equations for an inhomogeneous fluid (IEQ),[13] and density functional theory (DFT).[14] Although the MPB theory is quite successful in certain circumstances, the latter two approaches are the most satisfactory. More recently, we have returned to the study of the DL using MC simulations, DFT, and other theories. We have considered DLs formed by molten salts,[15] by aqueous electrolytes with strong ionic interactions,[16] and by ions at room temperature but with three different ion sizes (2, 3, and 4.25 Å).[17,18]

All the previously cited studies were performed using the primitive model (PM) of electrolytes, which consists of charged hard spheres, representing the ions, in a uniform dielectric medium that represents the solvent. Simulations using a molecular model of the solvent are much more difficult. For example, it is difficult to study anything but high concentrations, because the number of water molecules in a simulation becomes prohibitive at low concentrations. Regrettably, this limits the usefulness of the results, because one interesting result in a DL study is the dependence of the capacitance on concentrations, which requires a fairly broad range of concentrations. Nonetheless, several DL simulations[19−33] with explicit water molecules have been made.

In this work, we use the PM and continue our study of the effect of ion size in a DL by allowing the cations and anions to have different diameters and different charges. Because the smaller ions can approach the electrode more closely than larger ions, a charge separation occurs near the electrode that results in a nonzero potential, even if the electrode is uncharged, namely, at the point of zero (electrode) charge (PZC). This phenomenon is known and it was studied by Monte Carlo simulations,[8] the modified Gouy−Chapman (MGC) theory,[6,34] and the MSA.[38] The fact that a nonzero PZC potential appears even if the ions have the same diameter but different charge is less emphasized. Torrie et al.[9] described the effect with MC simulations and the MPB5 theory. They also investigated the influence of image effects on the PZC potential of 2:1

* Author to whom correspondence should be addressed. E-mail address: doug@chem.byu.edu.

10.1021/jp0473873 CCC: $27.50
Published on Web 09/29/2004

electrolytes. It seems that size asymmetry and charge asymmetry were studied separately by simulations and theories but not together. The main point of this work is to present the simultaneous effect of these two contributions. In some situations, these two effects enhance each other's influence, regarding the PZC potential, whereas in other cases, that influence is weakened.

We concentrate our efforts on the region of small electrode charge, because, as the electrode charge is increased, the nature of the DL is dominated by the counterions. As a result, the DL properties will become increasingly similar to those of a DL composed of cations and anions of the size and valence of the counterions. Thus, our main interest is the behavior of PZC potential for various values of the ion diameters, valences, and concentration.

A nonzero potential at the PZC is often taken as an indication of chemical interaction of the ions with the electrode, so there is value in knowing if this effect can result from other causes. This short-range interaction is different for the various ions (this phenomenon is termed "specific adsorption"), which results in a charge separation restricted to the surface of the electrode. From this charge separation, a potential difference follows. This contribution is thought to be, more or less, independent of concentration. The contribution that we study here is dependent on concentration, and it is a consequence of a charge separation in the diffuse layer. This separation of the PZC potential is slightly heuristic but a good starting point for our study, because specific adsorption is not included in our model: apart from hard-sphere exclusions, only electrostatic interactions act between the components of the system.

In this connection, it is important to realize that the results given here are likely to be an underestimate of the magnitude of the contribution of ion size and charge asymmetry. The effect can be enhanced by different ways. It is usual and is more similar to experimental situations to assign different DCA values for the different ions.[8] This approach is reasonable, because of the different ability of ions to disrupt the structure of solvent molecules near the electrode. Although the DCA need not be equal to the radius of the ions (as a matter of fact, generally they are not equal), in this work, we restrict ourselves to the case where the DCA is the ion radius needed to avoid the additional degrees of freedom in the model that would arise through empirical fitting. The case where ion radius and DCA are different will be considered in subsequent work, where we will compare with experiment. Note that a DCA that is different from the ion radius is easily incorporated into a simulation. It is less straightforward in a theory, because it corresponds to the nonadditivity of diameters. An analytic solution of an integral equation for nonadditive diameters can be quite difficult. A numerical solution is not so difficult. Of course, one can always displace density profiles in the spirit of the MGC theory for equal DCA but with unknown error and a loss of consistency.

Another effect that enhances the PZC potential can be the inclusion of dielectric boundaries in our system. If there is only one sharp dielectric interface at the boundary of the electrode and the electolyte, these effects can be taken into account by image charges.[5,8,9] Using a metallic electrode, the PZC potential is expected to be larger, because the smaller ions are drawn to the electrode by their stronger image charges.[8] Models of the DL where different dielectric constants are assigned to different layers of the electrolyte near the electrode can be constructed[39] and studied by our Induced Charge Computation method that was introduced recently.[40] It is our intention to study these effects in future work.

The term "double" layer is used for historical reasons. Simulations and modern theory have shown that there is layering in the charge profiles. This effect would be enhanced if explicit solvent molecules were present. The DL actually consists of many layers of differing charge. However, because the first counterion layer predominates, the term double layer is still appropriate.

2. Model

The model considered here is the PM of a binary electrolyte near a hard planar charged surface. The interaction between the ions of species i and j is that of the charged hard spheres:

$$u_{ij}(r) = \begin{cases} \infty & (\text{for } r < d_{ij}) \\ \dfrac{z_i z_j e^2}{\epsilon r} & (\text{for } r > d_{ij}) \end{cases} \tag{1}$$

where $d_{ij} = (d_i + d_j)/2$, e is the electron charge, ϵ is the dielectric constant of the solvent, z_i and d_i are the respective valence and diameter of the ion, and r is the distance of the two ions. We adopt the convention that species 2 is the species with the larger diameter. Here, we use $d_2 = 4.25$ Å and allow d_1 to vary within the range of 1.5−4.25 Å. We have considered simulations for size-symmetric electrolytes with such diameters in an earlier publication.[18] For ion valences, we use values in the range of 1−3 for the cations. The ion−electrode interaction is

$$u_i(x) = \begin{cases} \infty & (\text{for } x < d_i/2) \\ -\left(\dfrac{4\pi z_i e \sigma}{\epsilon}\right) x & (\text{for } x > d_i/2) \end{cases} \tag{2}$$

where σ is the charge density of the electrode and x is the distance of the ion from the electrode.

Poisson's equation is given as

$$\frac{\mathrm{d}^2\Phi(x)}{\mathrm{d}x^2} = -\frac{4\pi e}{\epsilon}\sum_i z_i \rho_i g_i(x) \tag{3}$$

where $\Phi(x)$ is the electric potential, $g_i(x) = \rho_i(x)/\rho_i$ is the dimensionless density profile of ions of species i, and $\rho_i = \rho_i(\infty)$ is the density far from the electrode. Integration of Poisson's equation yields

$$\frac{\mathrm{d}\Phi(x)}{\mathrm{d}x} = \begin{cases} \dfrac{4\pi e}{\epsilon}\displaystyle\sum_i z_i \rho_i \int_x^\infty g_i(t)\,\mathrm{d}t & (\text{for } d_2/2 < x < \infty) \\ \dfrac{4\pi e}{\epsilon}\left[z_2\rho_2\displaystyle\int_{d_2/2}^\infty g_2(t)\,\mathrm{d}t + z_1\rho_1\int_x^\infty g_1(t)\,\mathrm{d}t\right] & (\text{for } d_1/2 < x < d_2/2) \\ \dfrac{4\pi e}{\epsilon}\left[z_2\rho_2\displaystyle\int_{d_2/2}^\infty g_2(t)\,\mathrm{d}t + z_1\rho_1\int_{d_1/2}^\infty g_1(t)\,\mathrm{d}t\right] & (\text{for } 0 < x < d_1/2) \end{cases} \tag{4}$$

and

$$\Phi(x) = \begin{cases} -\frac{4\pi e}{\epsilon}\sum_i z_i\rho_i\int_x^\infty (t-x)g_i(t)\,dt & (\text{for } d_2/2 < x < \infty) \\ -\frac{4\pi e}{\epsilon}[z_2\rho_2\int_{d_2/2}^\infty (t-x)g_2(t)\,dt + & (\text{for } d_1/2 < x < d_2/2) \\ \quad z_1\rho_1\int_x^\infty (t-x)g_1(t)\,dt] & \\ -\frac{4\pi e}{\epsilon}[z_2\rho_2\int_{d_2/2}^\infty (t-x)g_2(t)\,dt + & (\text{for } 0 < x < d_1/2) \\ \quad z_1\rho_1\int_{d_1/2}^\infty (t-x)g_1(t)\,dt] & \end{cases} \quad (5)$$

In particular, the difference in potential across the DL is

$$\Phi(0) = -\frac{4\pi e}{\epsilon}[z_2\rho_2\int_{d_2/2}^\infty t g_2(t)\,dt + z_1\rho_1\int_{d_1/2}^\infty t g_1(t)\,dt] \quad (6)$$

Gaussian units have been used.

3. Monte Carlo Simulations

Our MC method is a slight modification of that of Torrie and Valleau,[4] which has been thoroughly discussed in their papers and in our previous papers. As a result, we will not repeat the details of the method. Briefly, we use a cell with periodic boundary conditions in the lateral (with respect to the surface of the electrode) directions. In the perpendicular direction, the cell is confined by a uniformly charged wall on the left and by a neutral hard wall on the right side.

A refined version[23] of the so-called charged sheet method[4] is used to treat the long-range contributions of the Coulombic forces. We use the canonical (constant *NVT*) ensemble; the dimension of the cell in the parallel direction must be large enough for a homogeneous fluid to exist in the middle of the cell. The desired concentration is obtained by performing a short pereliminary simulation and by modifying the cell size according to the obtained and desired bulk concentrations. The total charge of the cell is zero.

4. Modified Gouy−Chapman Theory

Twenty years ago, Valleau and Torrie[6] and Bhuiyan et al.[34] considered a MGC theory for electrolytes with asymmetric sizes by retaining the standard GC functional form but giving each ion a different DCA value (or Stern layer). A generalization of the MGC theory for any electrolyte stoichiometry has been proposed.[35] At best, this is a semi-satisfactory approach, because the ions in the GC theory are point ions without size. The MSA is thought to be preferable to the MGC theory, because ion size is incorporated in a natural and self-consistent manner. The MSA is a linearized theory and is applicable only for small electrode charge, whereas the MGC theory is not restricted to small electrode charge. However, because the region of small electrode charge is the most interesting region and because the MSA is restricted to the linear regime, we mention only the linearized version of the MGC theory in this paper.

For the linearized MGC theory (LMGC), the density profiles are given by

$$g_i(x) = u\left(x - \frac{d_i}{2}\right)[1 - \beta z_i e\Phi(x)] \quad (7)$$

where $u(x)$ is the unit step function and $\beta = 1/(kT)$ (where k is the Boltzmann constant and T is the temperature). For the potential, we provide an explicit analytic solution, which is given as

$$\Phi(x) = \begin{cases} \Phi(0) - \left(\frac{4\pi\sigma}{\epsilon}\right)x & (\text{for } x < d_1/2) \\ A_+e^{mx} + A_-e^{-mx} + \frac{1}{\beta z_1 e} & (\text{for } d_1/2 < x < d_2/2) \\ \Phi(d_2/2)e^{-\kappa(x-d_2/2)} & (\text{for } x > d_2/2) \end{cases} \quad (8)$$

with

$$\Phi(0) = \left(\frac{2\pi\sigma}{\epsilon}\right)d_1 + A_+e^{md_1/2} + A_-e^{-md_1/2} + \frac{1}{\beta z_1 e} \quad (9)$$

$$\Phi(d_2/2) = A_+e^{md_2/2} + A_-e^{-md_2/2} + \frac{1}{\beta z_1 e} \quad (10)$$

$$A_+ = \frac{-\left(\frac{\kappa}{\kappa - m}\right)\left(\frac{1}{\beta z_1 e}\right)e^{md_2/2} - \left(\frac{4\pi\sigma}{\epsilon m}\right)e^{md_1/2}}{\left(\frac{\kappa + m}{\kappa - m}\right)e^{md_2} + e^{md_1}} \quad (11)$$

$$A_- = \frac{-\left(\frac{\kappa}{\kappa + m}\right)\left(\frac{1}{\beta z_1 e}\right)e^{-md_2/2} + \left(\frac{4\pi\sigma}{\epsilon m}\right)e^{-md_1/2}}{\left(\frac{\kappa - m}{\kappa + m}\right)e^{-md_2} + e^{-md_1}} \quad (12)$$

κ is the Debye screening parameter,

$$\kappa^2 = \frac{4\pi\beta e^2}{\epsilon}\sum_i z_i^2\rho_i \quad (13)$$

and

$$m^2 = \frac{4\pi\beta e^2 z_1^2\rho_1}{\epsilon} \quad (14)$$

Solutions of the LMGC theory equivalent to that given in the aforementioned discussion have been published previously.[36,37] The interesting paper of Spitzer[37] includes dielectric boundaries in the model. We intend to study this phenomena in future MC simulations.

5. Mean Spherical Approximation

Density profiles are not available for the asymmetric size version of the MSA. Nonetheless, an expression for the electrode potential can be obtained.[38] It is

$$\Phi(0) = \frac{4\pi\sigma - 4ecB/D}{2\epsilon\Gamma} \quad (15)$$

where

$$c = \frac{\pi}{2}\left(1 - \frac{\pi}{6}\sum_i \rho_i d_i^3\right)^{-1} \quad (16)$$

$$\Gamma^2 = \frac{\pi\beta e^2}{\epsilon}\sum_i \rho_i X_i^2 \quad (17)$$

$$X_i = \frac{z_i - cBd_i^2/D}{1 + \Gamma d_i} \quad (18)$$

$$B = \sum_i \frac{z_i\rho_i d_i}{1 + \Gamma d_i} \quad (19)$$

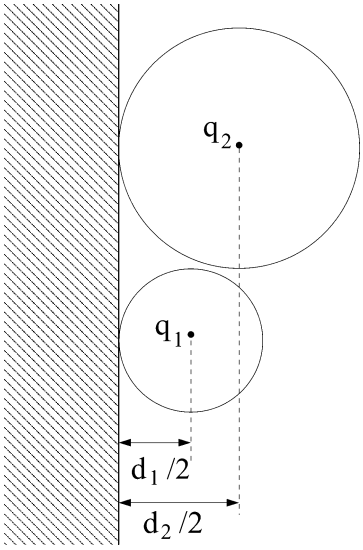

Figure 1. Schematic showing the geometry of the double layer.

and

$$D = 1 + c\sum_i \frac{\rho_i d_i^3}{1 + \Gamma d_i} \tag{20}$$

Currently, we are aware only of the works of Gillespie et al.[41,42] that have reported DFT results for ions of different size. Preliminary calculations[43] indicate that the method of these authors will predict the effects seen in this paper. Except for the MSA, there are no IEQ results for ions of different sizes. Even in the case of the MSA, we are aware only of results for integral quantities and we are not aware of any results for the density and potential profiles for ions of different size.

6. Results

Without any loss of generality, we have performed simulations for the case when the diameter of the cation is smaller than that of the anion (for the geometry, see Figure 1). Although this is the usual case for the ion diameters, we note that there is some experimental evidence that the DCA of an anion is smaller than that of a cation. The consequence of such a choice for the DCA value will be considered in a later publication. The reverse case (larger cation) is included in our results by changing the identity of the two ionic species. The diameter of the anion is fixed at a value of $d_2 = 4.25$ Å, and the diameter of the cation is changed in the range of 1.5−4 Å. In regard to the valence of the ions, we performed simulations for 1:1, 2:1, and 3:1 electrolytes.

Generally, we are interested in the behavior of the PZC potential; however, for some cases, voltage−charge curves are also presented. The concentrations that we consider are in the range of 0.0333−2 M. The temperature is $T = 300$ K, and the dielectric constant is characteristic of water: $\epsilon = 78.5$.

Figure 2 shows the dependence of the PZC potential from the ratio of the diameters of the cation and the anion for 1:1 electrolytes. The symbols, the dashed curves, and solid curves represent MC, LMGC, and MSA data, respectively. $\Phi(0)$ increases as the size asymmetry increases, and $\Phi(0) = 0$ if $d_1 = d_2$. Because the positive ions can approach the electrode more closely, the PZC potential is positive, and it becomes more positive as the concentration is increased. Interestingly, the agreement of the simulation is much better with the LMGC results than with the MSA results. MSA gives satisfactory results

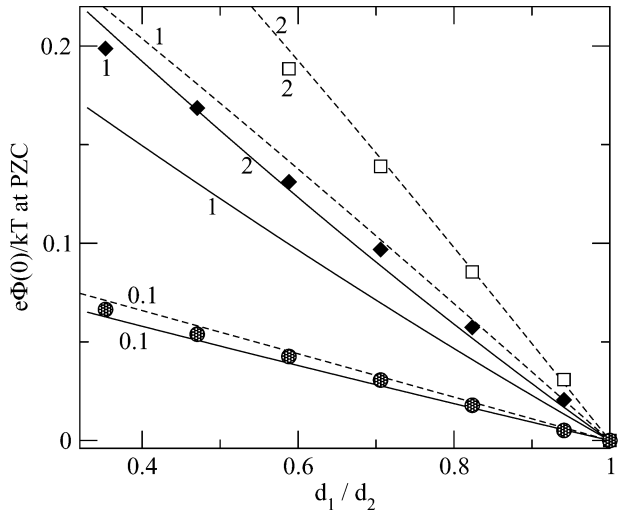

Figure 2. Graph of the PZC potential as a function of the ratio of diameters of the cation and the anion for 1:1 electrolytes. The symbols, solid lines, and dashed lines show the Monte Carlo (MC), mean spherical approximation (MSA), and linearized modified Gouy−Champan (LMGC) results, respectively; the numbers near the lines and symbols denote concentrations measured in molarity (M).

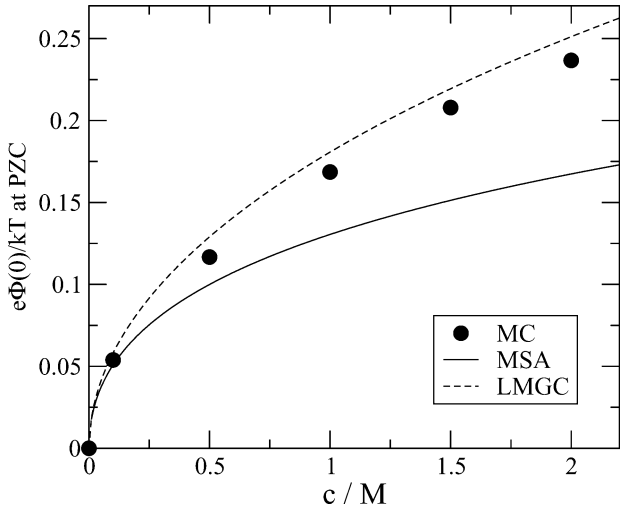

Figure 3. Graph of the PZC potential as a function of the concentration for a diameter ratio of $d_1/d_2 = 0.471$ for a 1:1 electrolyte obtained from different methods. The meanings of the curves and symbols are the same as those given in Figure 2.

only for low concentration, whereas the LMGC theory works quite well, even for high concentrations. The concentration dependence, as obtained from different methods, can be seen in Figure 3 for the diameter ratio $d_1/d_2 = 0.471$.

Figure 4 shows the voltage−charge curves for the ion diameter ratio $d_1/d_2 = 0.471$ for a large concentration (1 M) and a small concentration (0.1 M). The difference between MSA and LMGC is less clear: both theories reproduce the slope of the $\Phi(0)$ vs σ curves (the capacitance of the DL) well, although the MSA gives better results for the slope (the slopes are 61.32, 61.21, and 62.22 for MC, MSA, and LMGC, respectively, for 0.1 M). In contrast, as observed previously, the potential at $\sigma = 0$ is reproduced better by the LMGC theory, although it is less apparent on the scale of this figure.

The cases of 2:1 and 3:1 electrolytes are considered in Figures 5 and 6. The most striking feature of the figures is that the MC data are shifted toward more-negative values of the PZC potential. The PZC potential has a relatively large negative value for $d_1 = d_2$, namely, charge asymmetry itself is able to produce

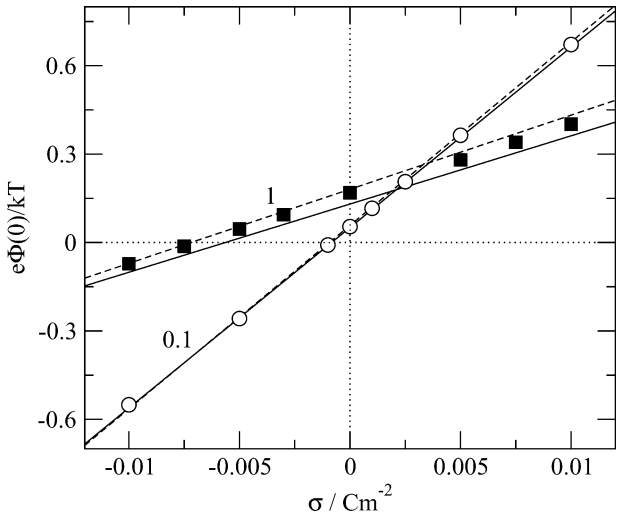

Figure 4. Graph of the electrode potential as a function of the electrode charge for 1:1 electrolytes for two different concentrations (0.1 and 1 M; see the numbers near the curves). The ratio of the ionic diameters is $d_1/d_2 = 0.471$, and the meanings of the curves and symbols are the same as those given in Figure 2.

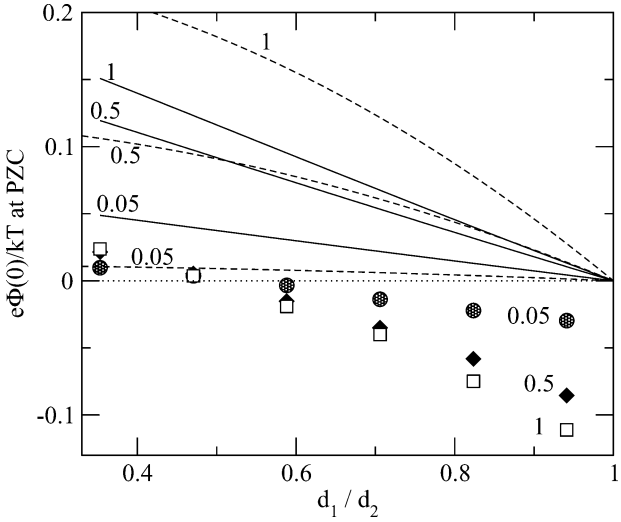

Figure 5. Graph of the PZC potential as a function of the ratio of diameters of the cation and the anion for 2:1 electrolytes. The meanings of the curves and symbols are the same as those given in Figure 2, and the numbers near the lines and symbols denote concentrations (in units of M).

a double layer and a potential. For the 3:1 case, we did not even find a diameter ratio where the positive potential resulting from the size asymmetry can overcome the negative potential resulting from the charge asymmetry. For the 2:1 case, the two effects have a tendency to cancel each other at a diameter ratio of $d_1/d_2 \approx 0.471$. Interestingly, the point where this cancellation occurs seems to be independent of the concentration.

In regard to the ability of the theories to reproduce the MC data, the situation is worse for the 2:1 and 3:1 electrolytes than for the 1:1 case. The LMGC and MSA theories are not able to reproduce the negative PZC potential term resulting from the charge asymmetry: both MSA and LMGC theories (and also DFT in its present form) produce a zero PZC potential if $d_1 = d_2$. To our knowledge, only the MPB5 theory is known to reproduce this phenomenon.[9]

The competition of the size and charge asymmetry can be seen from the behavior of the PZC potential (Figure 7). The potentials are monotonic for the 1:1 case when there is no charge asymmetry. In the 2:1 case, where the two effects have a similar

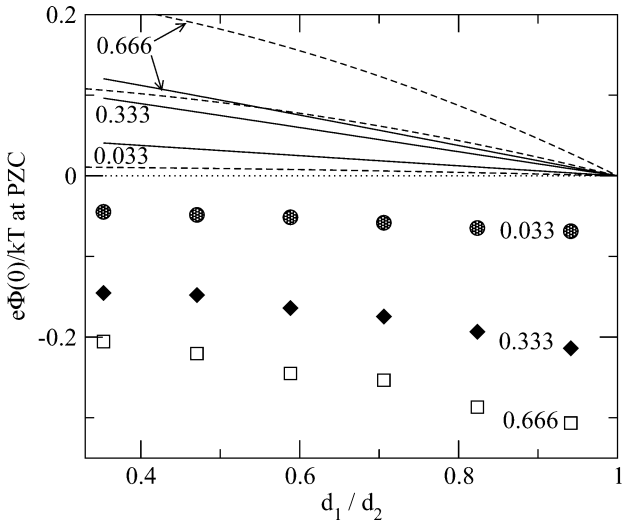

Figure 6. Graph of the PZC potential as a function of the ratio of diameters of the cation and the anion for 3:1 electrolytes. The meanings of the curves and symbols are the same as those given in Figure 2. The numbers near the lines and symbols denote concentrations (in units of M).

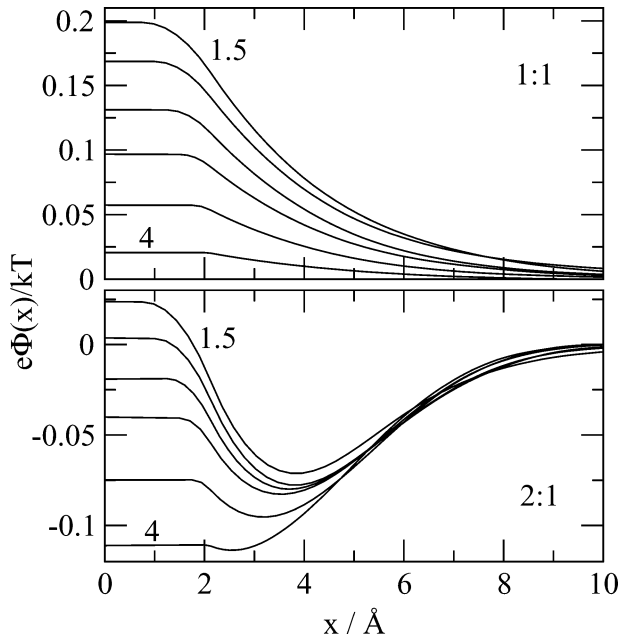

Figure 7. Graph of the PZC potential as a function of the distance from the electrode for a 1 M electrolyte. The diameter of the anion is fixed at a value of $d_2 = 4.25$ Å, whereas the cation diameters range over the values of $d_+ = 1.5$, 2, 2.5, 3, 3.5, and 4 Å inside a given inset. Numbers near curves denote cation diameters. Top and bottom panels refer to 1:1 and 2:1 electrolytes, respectively.

magnitude, an oscillation occurs in the potential profiles. The charge asymmetry causes a longer-range effect than does the size asymmetry. As the electrode is approached, the charge asymmetry brings the potential down toward negative values. However, closer to the electrode, the effect of the size asymmetry appears, which takes the potential toward more-positive values. In the 3:1 case, for which potential profiles are not shown, the charge asymmetry dominates.

The voltage−charge relationship for the 2:1 case can be observed in Figure 8. The diameter ratio is $d_1/d_2 = 0.471$. Coincidentally, this is near the ratio where the charge and size asymmetries almost cancel each other. The fact that this cancellation occurs when the charge of the cation is twice the magnitude of the charge of the anion while its diameter is

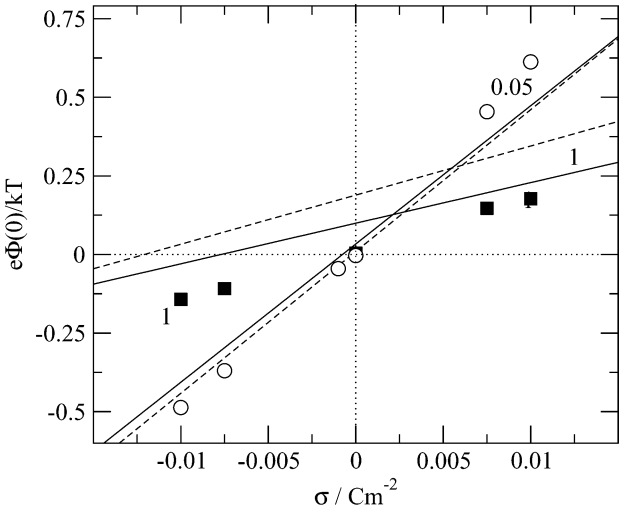

Figure 8. Graph of the electrode potential as a function of the electrode charge for 2:1 electrolytes for two different concentrations (0.1 and 1 M; see the numbers near the curves and symbols). The ratio of the ionic diameters is $d_1/d_2 = 0.471$, and the meanings of the curves and symbols are the same as those given in Figure 2.

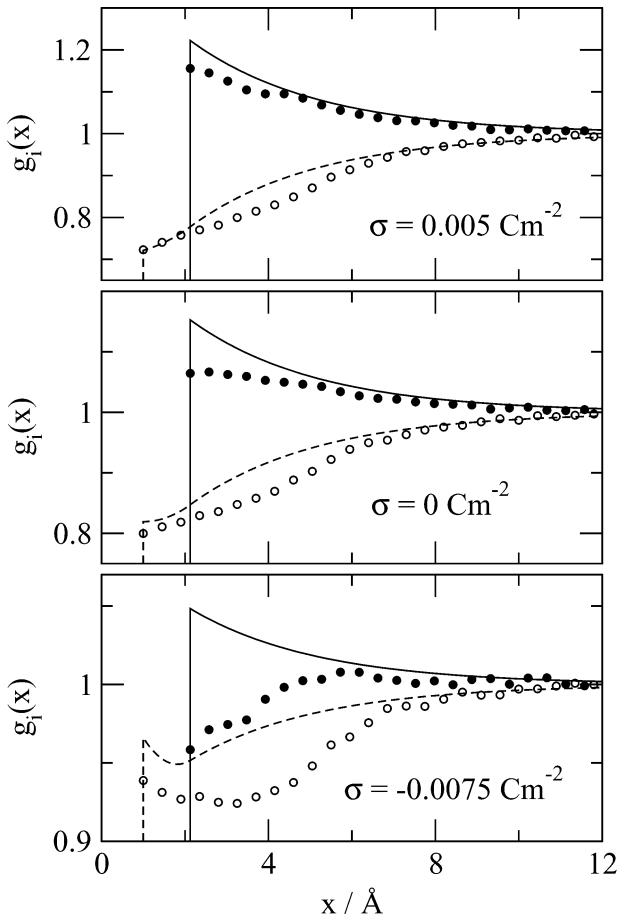

Figure 9. Normalized density profiles for 1:1 electrolytes for three different electrode charges as obtained from simulation (open and filled symbols for cations and anions, respectively) and the LMGC theory (dashed and solid curves for cations and anions, respectively). The ratio of the ionic diameters is $d_1/d_2 = 0.471$, and the concentration is 1 M.

approximately half of that of the anion is probably a coincidence. In this situation, the theories do not work very well, as is expected from the earlier results (i.e., see Figure 4).

The LMGC theory, as presented in this paper, provides explicit analytic formulas for the density and potential profiles. Therefore, a comparison with the simulation results is worthwhile. Figure 9 shows density profiles for the 1:1 case at a given diameter ratio and concentration. The various insets of the figure show results for different electrode charges. Figure 10 shows the potential profiles for the same situations. At $\sigma = 0.005$ C/m^2, the electrode potential is positive, and the density and potential curves show very good agreement. At zero charge, the simulation density profiles decline close to the electrode (drying). The LMGC curves cannot reproduce this behavior. This is more apparent for the negative electrode charge of $\sigma = -0.0075$ C/m^2. Drying influences both cations and anions to approximately the same degree; therefore, the difference of the profiles is not affected, as shown in Figure 11. The potential is dependent on the difference of the profiles; therefore, the potential profiles are also only slightly affected by the errors in the density profiles (see Figure 10).

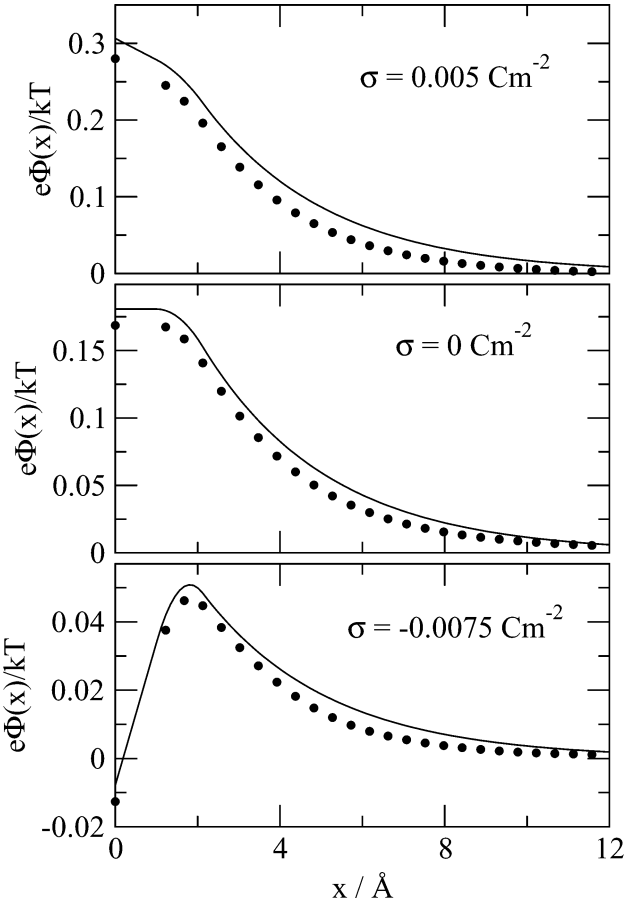

Figure 10. Potential profiles for 1:1 electrolytes for three different electrode charges, as obtained from simulation (symbols) and the LMGC theory (curves). The ratio of the ionic diameters is $d_1/d_2 = 0.471$, and the concentration is 1 M.

Figure 12 shows density and potential profiles for a 2:1 electrolyte at the PZC. At this point, the MC method gives a negative PZC potential, whereas the potential obtained from the LMGC theory is positive. The density profiles indicate that a layer with an excess of small cations appears close to the electrode. A second layer of the large anions then follows. In the case of the simulation profiles, a third layer of cations appears that is absent in the case of the LMGC theory. This layering that appears further from the electrode is a consequence of the charge asymmetry and it makes the PZC potential more negative. The LMGC theory is unable to reproduce these features.

Although, on the basis of the results presented in this paper, charge asymmetry seems to be quite important, the importance

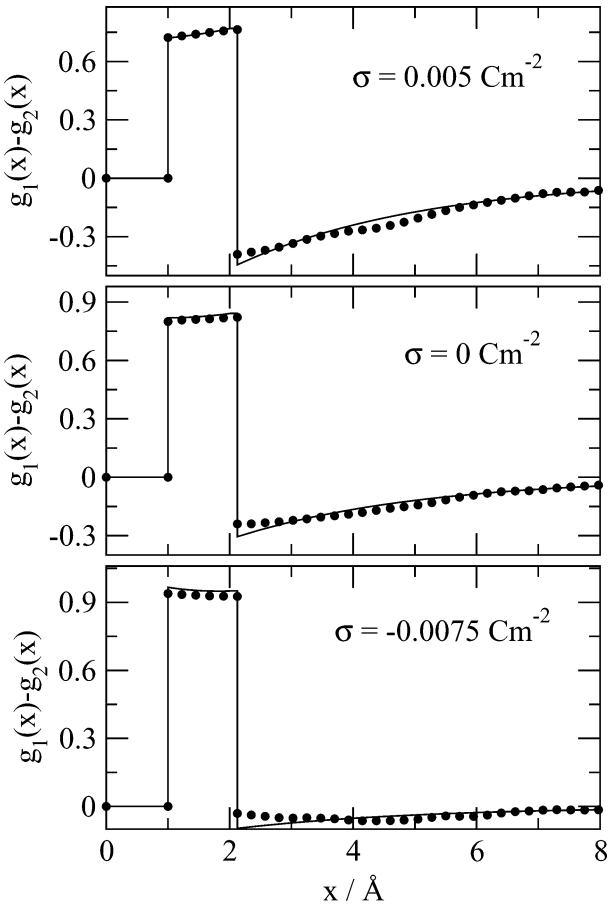

Figure 11. Difference of the density profiles for 1:1 electrolytes for three different electrode charges, as obtained from simulation (symbols) and the LMGC theory (curves). The ratio of the ionic diameters is $d_1/d_2 = 0.471$, and the concentration is 1 M.

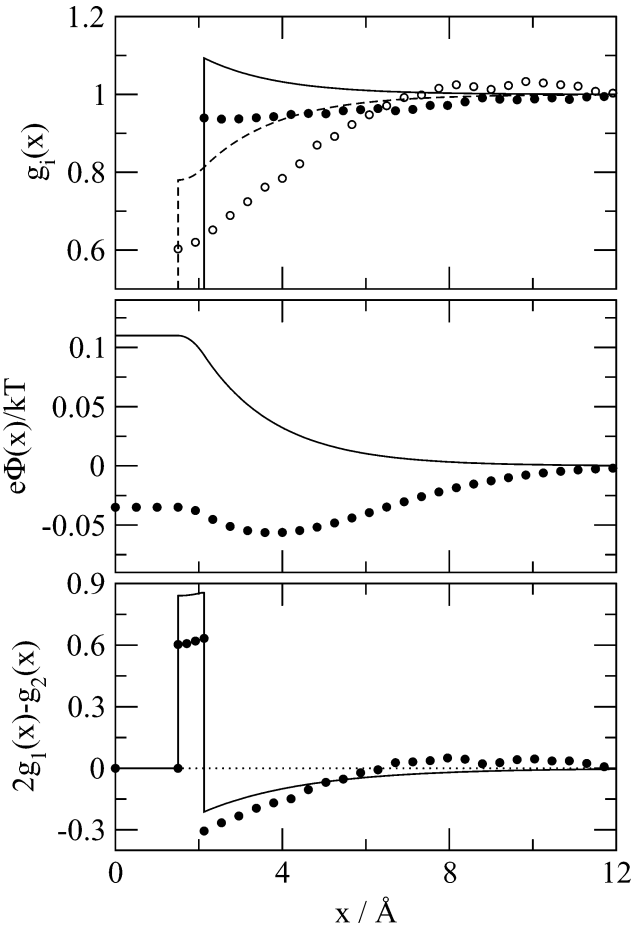

Figure 12. Normalized density (the meanings of the curves and symbols is the same as in Figure 9), potential and density difference profiles for 2:1 electrolytes for zero electrode charge, as obtained from simulation (symbols) and the LMGC theory (curves). The ratio of the ionic diameters is $d_1/d_2 = 0.706$, and the concentration is 0.5 M.

of the size asymmetry cannot be overestimated. It can give a large contribution for ions with a large difference in diameter. Moreover, for the PZC potential, the DCA is a more important quantity than the ionic diameters. Using different DCA values for the various ions that are obtained from experiment or explicit solvent simulations, we can reach a better understanding of the experimental behavior of the PZC potential of electrical DLs.

7. Summary

At high electrode charge, the dominant part of the double layer (DL) near the electrode consists of counterions. As a result, the simulation data must merge into the previously reported results for a DL formed by a symmetric electrolyte where the ionic diameter is equal to that of the counterions. At low electrode charge, the simulation results differ qualitatively as well as quantitatively from those reported for equal size ions by Torrie and Valleau and by us. At low electrode charge, the shift in the potential can be seen clearly, because it is not obscured by the potential of the electrode/counterion DL that dominates at high electrode charges.

There is a nonzero potential, even when the electrode is uncharged. This nonzero point of zero charge (PZC) potential arises if either the diameter or the charge of the ions (or both) are different. In this paper, our main emphasis is on studying the competition that appears between the size and charge asymmetry of the ions. These effects sometimes enhance (and sometimes weaken) each other.

The effect of size asymmetry can be added to the Gouy-Champan (GC) theory, even though it is a theory of point ions, by giving the cations and anions a different distance of closest approximation (DCA) (Stern layer). The effect of size asymmetry arises more naturally in the mean spherical approximation (MSA). Despite this observation, the linearized modified Gouy−Champan (LMGC) theory is better in regard to reproducing the potential shift due to size asymmetry of the ions. The potential due to charge asymmetry cannot be reproduced by either the LMGC or MSA theories.

The fact that the LMGC theory results are more accurate for monovalent ions is surprising, because the conventional wisdom is that the MSA is preferable to the LMGC theory, because the MSA treats ion size in a self-consistent manner, in contrast to the LMGC theory, in which ion size is ignored, except for the DCA of the ions. One must be circumspect in making this statement, because it is possible that there is an error in the paper by Khater et al.[38] Also two caveats should be kept in mind. First, there is nothing magical about monovalent ions. Monovalent ions at a lower temperature or in a lower dielectric solvent will behave as multivalent ions. Second, just because the LMGC theory is better at predicting the potential shift due to size asymmetry does not make it a good theory for monovalent ions. In the linear regime, the LMGC theory overestimates the increase in the potential as a function of electrode charge, whereas the MSA is more successful for this property.

A few simulations for 2:2 electrolytes have shown that the PZC potential is zero if $d_1 = d_2$, namely, that it is really the

charge asymmetry that causes a potential shift, and not simply the stronger interaction between the ions.

A nonzero potential at the PZC is often taken as a signature of specific or chemical adsorption. If we assume that the concentration-independent part of the PZC potential corresponds to specific short-range interactions between the electrode and the ions and that the diffuse layer studied in this work is responsible for the concentration-dependent part, we can relate our Monte Carlo (MC) results to experimental situations. This work is underway.

Acknowledgment. This work was supported in part by a NATO Collaborative Linkage Grant (No. PST.CLG.980366). The use of the facilities of the Ira and Marylou Fulton Supercomputing Center at BYU is acknowledged with thanks.

References and Notes

(1) Gouy, G. *J. Phys.* **1910**, *9*, 457.
(2) Chapman, D. L. *Philos. Mag.* **1913**, *25*, 475.
(3) Blum, L. *J. Phys. Chem.* **1977**, *81*, 136.
(4) Torrie, G. M.; Valleau, J. P. *J. Chem. Phys.* **1980**, *73*, 5807.
(5) Torrie, G. M.; Valleau, J. P.; Patey, G. N. *J. Chem. Phys.* **1982**, *76*, 4615.
(6) Valleau, J. P.; Torrie, G. M. *J. Chem. Phys.* **1982**, *76*, 4623.
(7) Torrie, G. M.; Valleau, J. P. *J. Phys. Chem.* **1982**, *86*, 3251.
(8) Valleau, J. P.; Torrie, G. M. *J. Chem. Phys.* **1984**, *81*, 6291.
(9) Torrie, G. M.; Valleau, J. P.; Outhwaite, C. W. *J. Chem. Phys.* **1984**, *81*, 6296.
(10) Outhwaite, C. W.; Bhuiyan, L. B. *J. Chem. Soc., Faraday Trans.* **1983**, *79*, 707.
(11) Henderson, D.; Blum, L.; Smith, W. R. *Chem. Phys. Lett.* **1979**, *63*, 381.
(12) Lozada-Cassou, M.; Saavedra-Barrera, R.; Henderson, D. *J. Chem. Phys.* **1982**, *77*, 1472.
(13) Plischke, M.; Henderson, D. *J. Chem. Phys.* **1988**, *88*, 2712.
(14) Rosenfeld, Y. *J. Chem. Phys.* **1993**, *109*, 8126.
(15) Boda, D.; Henderson, D.; Chan, K.-Y. *J. Chem. Phys.* **1999**, *110*, 5346.
(16) Boda, D.; Henderson, D.; Chan, K.-Y.; Wasan, D. T. *Chem. Phys. Lett.* **1999**, *308*, 473.
(17) Boda, D.; Fawcett, W. R.; Henderson, D.; Sokołowski, S. *J. Chem. Phys.* **2002**, *116*, 7170.
(18) Boda, D.; Henderson, D.; Plaschko, P.; Fawcett, W. R. *Mol. Simul.* **2004**, *30*, 137.
(19) Philpott, M. R.; Glosli, J. N. *J. Electrochem. Soc.* **1995**, *142*, L25.
(20) Philpott, M. R.; Glosli, J. N.; Zhu, S.-B. *Surf. Sci.* **1995**, *335*, 422.
(21) Philpott, M. R.; Glosli, J. N. *J. Electroanal. Chem.* **1996**, *409*, 65.
(22) Philpott, M. R.; Glosli, J. N. *ACS Symp. Ser.* **1997**, *656*, 13.
(23) Boda, D.; Chan, K.-Y.; Henderson, D. *J. Chem. Phys.* **1998**, *109*, 1362.
(24) Spohr, E. *J. Electroanal. Chem.* **1998**, *450*, 327.
(25) Spohr, E. *Electrochim. Acta* **1999**, *44*, 1697.
(26) Spohr, E. *Electrochim. Acta* **2003**, *49*, 23.
(27) Crozier, P. S.; Rowley, R. L.; Henderson, D. *J. Chem. Phys.* **2001**, *114*, 7513.
(28) Crozier, P. S.; Rowley, R. L.; Henderson, D. *J. Chem. Phys.* **2002**, *113*, 9202.
(29) Dimitrov, D. I.; Raev, N. D. *J. Electroanal. Chem.* **2000**, *486*, 1.
(30) Dimitrov, D. I.; Raev, N. D.; Semerdzhiev, K. I. *Phys. Chem. Chem. Phys.* **2001**, *3*, 44.
(31) Guymon, C. G.; Hunsaker, M. L.; Harb, J N.; Henderson, D.; Rowley, R. L. *J. Chem. Phys.* **2003**, *118*, 10195.
(32) Stöckelmann, E.; Hentsche, R. *J. Chem. Phys.* **1999**, *110*, 12097.
(33) Stöckelmann, E.; Hentsche, R. *Langmuir* **2002**, *18*, 547.
(34) Bhuiyan, L. B.; Blum, L.; Henderson, D. *J. Chem. Phys.* **1983**, *78*, 442.
(35) Andreu, R.; Molero, M.; Calvente, J. J.; Carbaja, J. *J. Electroanal. Chem.* **1993**, *358*, 49.
(36) Grimson, M. J. *Chem. Phys. Lett.* **1983**, *95*, 426.
(37) Spitzer, J. J. *J. Colloid Interface Sci.* **1983**, *92*, 198.
(38) Khater, A. F.; Henderson, D.; Blum, L.; Bhuiyan, L. B. *J. Phys. Chem.* **1984**, *88*, 3682.
(39) Boda, D.; Nagy, T.; Gillespie, D.; Henderson, D. *J. Chem. Phys.* **2004**, submitted.
(40) Boda, D.; Gillespie, D.; Nonner, W.; Henderson, D.; Eisenberg, B. *Phys. Rev. E* **2004**, *69*, 046702.
(41) Gillespie, D.; Nonner, W.; Eisenberg, R. S. *J. Phys.: Condens. Matter* **2002**, *14*, 12129.
(42) Gillespie, D.; Nonner, W.; Eisenberg, R. S. *Phys. Rev. E* **2003**, *68*, 031503.
(43) Gillespie, D. Private communication.